

Electron-Transfer-Induced Diels–Alder Reactions of Indole and Exocyclic Dienes: Synthesis and Quantum-Chemical Studies

Udo Haberl,^[a] Eberhard Steckhan,*^[a] Siegfried Blechert,^[b] and Olaf Wiest^[c]

Abstract: Photoinduced electron transfer (PET) initiates radical-cation Diels–Alder reactions between indole and exocyclic dienes. As catalysts, triarylpyrylium tetrafluoroborates are used. The products are [*b*]-anellated tetrahydrocarbazoles, which are not accessible through neutral cycloadditions. The resulting structures are of interest because of their DNA intercalating properties, their antitumor activity, and their importance as building blocks of numerous indole alkaloids. When the exocyclic dienes are substituted with an aromatic

or heteroaromatic ring, the reaction proceeds with complete regioselectivity. The mechanism is discussed in detail and the potential-energy hypersurface of the radical-cation Diels–Alder reaction is investigated with quantum-chemical methods by variation of the distances of the two newly formed bonds. The

potential surface demonstrates the non-synchronous and nonconcerted reaction pathway. The energies of the different long-bond intermediates, which are local minima on the energy surface, have been calculated with semiempirical, molecular orbital, and density functional methods. Regio- and diastereoselectivities can be explained and predicted by comparing these energies. Quantum-chemical calculations lead to a reaction model that is consistent with the observed products.

Keywords: ab initio calculations • cycloadditions • density functional theory • electron transfer • radical ions

Introduction

Electron-transfer-induced [4+2] cycloadditions have proved to be a promising tool for organic synthesis and have been reviewed several times.^[1] Electron transfer, as the most simple method for a redox umpolung, permits cycloadditions between reactants with similar HOMO energies under mild conditions via electrochemically, photochemically, or chemically generated radical cations. These radical-cation-initiated reactions have reaction rates several orders of magnitude greater than that of the corresponding neutral reactions owing to a very low activation barrier.

Recently, we demonstrated the advantage of radical-cation cycloadditions with heterocyclic compounds with numerous examples.^[2] The efficient applicability of this reaction to the synthesis of natural products could also be demonstrated.^[3] The mechanism of the radical-cation Diels–Alder reaction is much less understood than that of the neutral version. This lack of basic understanding is not only unsatisfactory from a scientific point of view, but also hinders the development of synthetic applications of electron transfer catalysis. In particular, the laws underlying the often excellent regioselectivity are not understood.

Under conventional reaction conditions, indole, as an electron-rich heteroaromatic compound, does not react as a dienophile in a normal electron-demand Diels–Alder reaction because of the big HOMO–LUMO gaps. This cycloaddition with very electron-deficient compounds only takes place under very drastic conditions.^[4] Lewis acid catalysis is usually not effective because indoles are prone to rapid polymerization. We demonstrated the very efficient application of indole and its derivatives in electron-transfer-induced Diels–Alder reactions.^[5] In these studies, we found regioselective radical-cation Diels–Alder reactions of indole and monosubstituted exocyclic dienes. The resulting [*b*]-anellated tetrahydrocarbazoles structures, such as ellipticines, have been studied extensively owing to their antitumor activity.^[6]

The mechanistic aspects of the radical-cation Diels–Alder reaction of simple hydrocarbons have been investigated in

[a] Prof. Dr. E. Steckhan, Dipl.-Chem. U. Haberl
Kekulé-Institut für Organische Chemie und Biochemie
Universität Bonn, Gerhard-Domagk-Str. 1, D-53121 Bonn (Germany)
Fax: (+49) 228-735683
E-mail: steckhan@uni-bonn.de
haberl@uni-bonn.de

[b] Prof. Dr. S. Blechert
Institut für Organische Chemie, Technische Universität Berlin
Strasse des 17. Juni 124, D-10623 Berlin (Germany)
Fax: (+49) 30-31423619
E-mail: sibl@wap0105.chem.tu-berlin.de

[c] Prof. Dr. O. Wiest
Department of Chemistry and Biochemistry
University of Notre Dame
Notre Dame, IN 46556 (USA)
Fax: (+1) 219-6316652
E-mail: wiest.1@nd.edu

detail.^[7] Computational investigations suggest a nonsynchronous cycloaddition.^[8–10] Theoretical interest has focused on the high regioselectivities of this reaction type.^[8] The predictive power of the frontier molecular orbital (FMO) theory for this reaction is limited, because it is usually not clear which of the three possible interactions (HOMO–SOMO, SOMO–LUMO and HOMO–LUMO) is dominant. The failure of the FMO models is exemplified by the “role selectivity” model^[11] that was disproven experimentally.^[12]

As a result of their redox umpolung characteristics, the radical-cation-initiated cycloaddition reactions are of high synthetic value. However, they are still lacking predictability. Therefore, the development of rules that allow the prediction of substituent effects, regiochemistry, stereochemistry, and so forth would provide a broader basis for the application of this powerful method for the catalysis of slow or symmetry-forbidden pericyclic reactions. Computational chemistry is advantageous for the study of this reaction and the development of such rules, because the otherwise necessary experimental data are difficult to obtain owing to the extremely short lifetime of the species involved in the reaction mechanism.

This paper presents the first combination of experimental and theoretical DFT studies of substituent effects in radical-cation Diels–Alder reactions. The calculations are successfully applied to explain and to predict the regio- and stereoselectivities of the performed experiments and allow the study of the potential-energy surfaces for this reaction type. The minimum-energy reaction pathway on the potential-energy surface can thus be determined.

Abstract in German: Photochemisch induzierter Elektronentransfer (PET) initiiert Radikalkationen-Diels–Alder-Reaktionen zwischen Indol und exocyclischen Dienen. Als Katalysatoren werden Triarylpyrylium-tetrafluoroborate eingesetzt. Die Produkte sind [b]-annellierte Tetrahydrocarbazole, die über die entsprechenden neutralen Cycloadditionen nicht zugänglich sind. Die resultierenden Strukturen sind wegen ihrer DNA-interkalierenden Eigenschaften, ihrer Antitumor-Aktivität und wegen ihrer Bedeutung als Bestandteil zahlreicher Indol-Alkaloide von Interesse. Bei Substitution der exocyclischen Diene mit einem aromatischen oder heteroaromatischen Ring verläuft die Reaktion mit vollständiger Regio-selektivität. Der Mechanismus wird ausführlich diskutiert und die Energiehyperfläche der Radikalkationen-Diels–Alder-Reaktion wird mit quantenchemischen Methoden unter Variation der Abstände der beiden neu gebildeten Bindungen untersucht. Die Energiehyperfläche veranschaulicht den nicht-synchronen und nicht-konzertierten Reaktionsverlauf. Die Energien der verschiedenen „long-bond“-Intermediate, die lokale Minima auf der Hyperfläche darstellen, wurden mit semiempirischen, Molekülorbital- und Dichtefunktionalmethoden berechnet. Durch den Vergleich dieser Energien können die Regio- und Diastereoselektivitäten erklärt und vorhergesagt werden. Die quantenchemischen Rechnungen führen zu einem Reaktionsmodell, das in Einklang mit den beobachteten Produkten steht.

Results and Discussion

Cycloadditions between indole and aryl- or furyl-substituted exocyclic dienes by photoinduced electron transfer: A radical-cation [4+2]-cycloaddition reaction occurs between two compounds of nearly identical HOMO energies by a redox umpolung of either the diene or the dienophile to the corresponding radical cation. We have shown earlier that for an efficient reaction, the oxidation potentials of the diene and the dienophile should not differ by much more than 500 mV.^[8] This corresponds to the fact that the HOMO energies of the diene and the dienophile should not differ by more than 0.6 eV. The calculation of HOMO energies with the RHF/AM1 method provides a very efficient method to find appropriate reaction partners for the radical-cation Diels–Alder reaction.^[13] Therefore, we chose the exocyclic dienes **2**, **3**, and **4** as suitable reaction partners for a reaction with indole (**1**), which has a calculated HOMO energy of -8.40 eV (Figure 1). These unsymmetrically monosubstituted exocyclic dienes are good candidates for the investigation of the regioselectivity and the stereoselectivity of the cycloaddition.

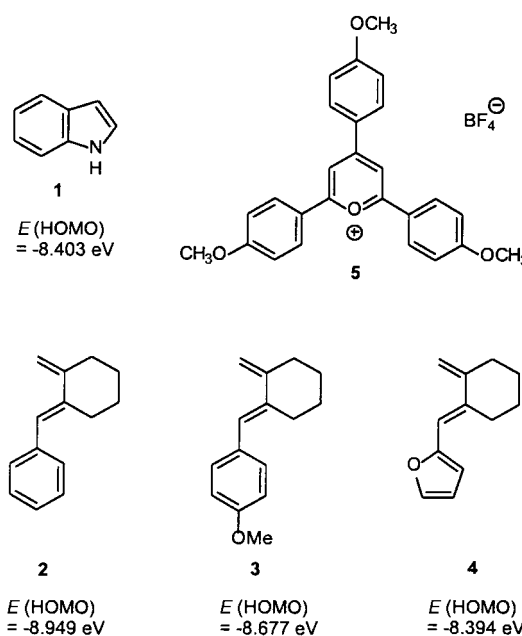
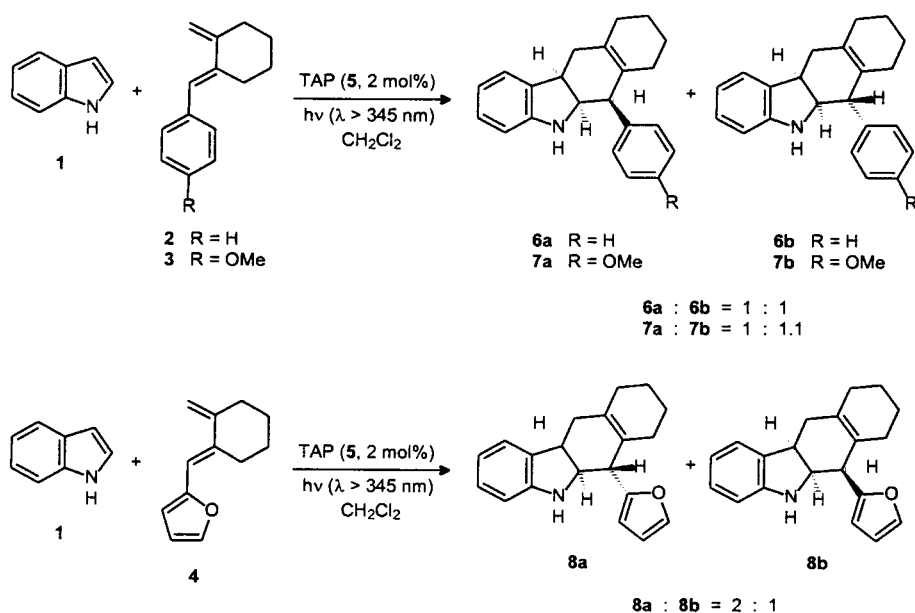


Figure 1. Starting materials and sensitizer for the photochemically induced radical-cation Diels–Alder reactions.

All reactions were performed by using 1–2 mol % of 2,4,6-tris(4-methoxyphenyl)pyrylium tetrafluoroborate (TAP, **5**) as sensitizer. Irradiation took place by means of a xenon arc lamp with the wavelengths filtered to values above 345 nm.

The phenyl-substituted exocyclic diene **2**, which has a calculated HOMO energy of -8.949 eV, reacts with indole with complete regioselectivity to give diastereomers **6a** and **6b** in a ratio of 1:1 as the only products with 28% yield (Scheme 1).

The exocyclic diene **3** with a 4-methoxy group at the phenyl ring has a calculated HOMO energy of -8.677 eV. The methoxy group has the effect that diene **3** has a smaller HOMO energy difference to indole than diene **2** and, thus, the



Scheme 1. Reactions of indole with aryl-substituted exocyclic dienes **2** and **3** and with furyl-substituted exocyclic diene **4**.

cycloaddition with **3** results in better yields (36%) than the reaction with diene **2**. The reaction is also completely regioselective and the diastereomers **7a** and **7b** are formed in a ratio of 1:1.1.

The substitution of the phenyl group with a furan ring in the exocyclic diene (**4**) leads to the preferred formation of diastereomer **8a** (Scheme 1). The diene **4** has a calculated HOMO energy of -8.394 eV and is therefore a good reaction partner for a radical-cation reaction with indole. In this case, the diastereomers **8a** and **8b** are formed in a ratio of 2:1 with 46% yield in contrast to the 1:1 ratios found for **6** and **7**. The structures of all diastereomers in this paper have been proved by NOE ^1H NMR experiments. The increase of intensity of the signals caused by pairs of hydrogen atoms through saturation of the corresponding NMR frequencies is indicated by double arrows in Figure 2 with compounds **6a** and **6b** as an example.

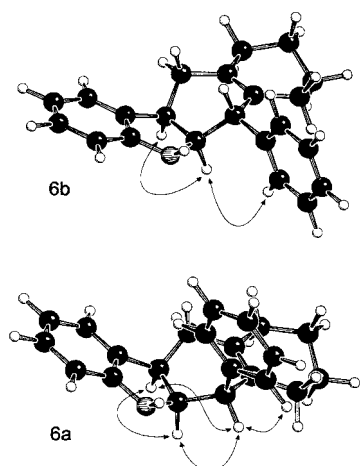


Figure 2. Determination of the configuration of the diastereomers by NOE.

Potential-energy surfaces: The absence of general rules that predict the regiochemistry and stereochemistry of the radical-cation Diels–Alder reaction leads to a high demand for a theoretical model based on detailed quantum-chemical calculations of the reaction mechanism. Closer insight into the mechanism of these reactions is necessary for the explanation and prediction of the observed regio- and diastereoselectivities. The paradox lies in the fact that radical and radical-ion pericyclic reactions are forbidden in the Woodward–Hoffmann sense because the symmetry of the singly occupied molecular orbital (SOMO) changes from reactant to product. In earlier theoretical studies, a non-

concerted mechanism via long-bond intermediates was calculated for radical-cation Diels–Alder reactions.^[8] To compare a synchronous with a nonsynchronous reaction path, we calculated a complete potential-energy surface (Figure 3) of this reaction type by variation of the distances (x and y) of the two newly formed bonds in the radical cation (Scheme 2). These

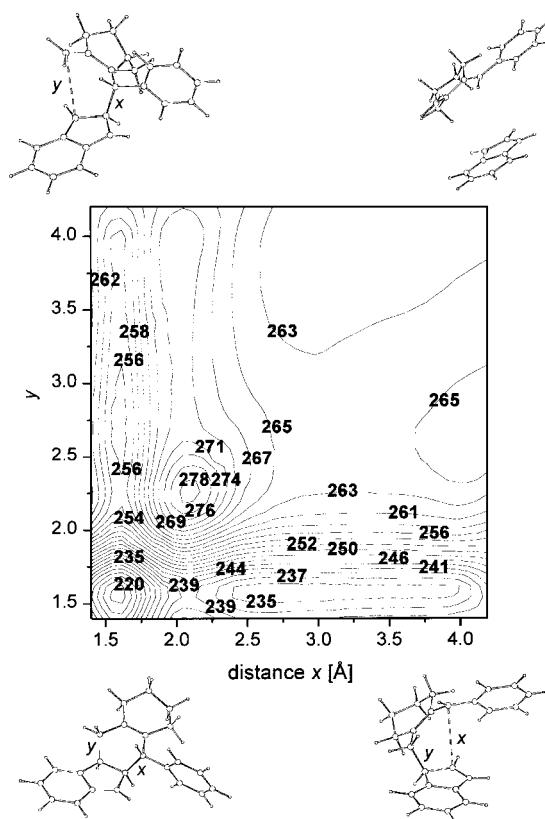
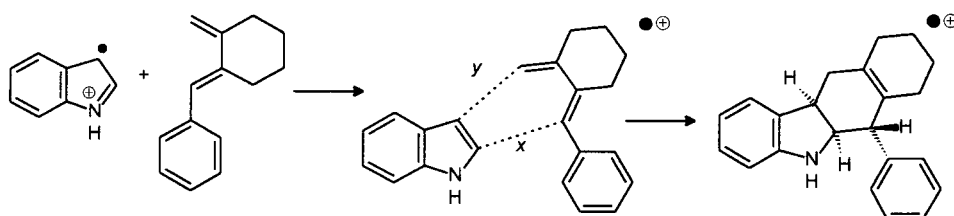


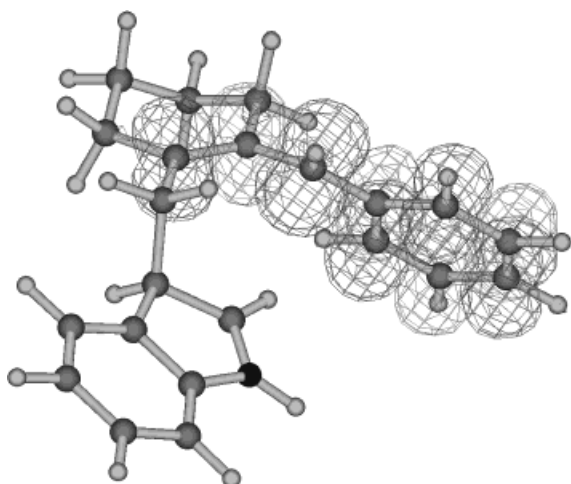
Figure 3. Contour plot of the potential-energy surface of the formation of **6b**. The energy values are given in kcal mol^{-1} .

Scheme 2. Variation of the distances x and y on the potential energy surface.

calculations were carried out with the UHF/AM1 method with complete geometry optimization on every point. DFT calculations of the stationary points on this hypersurface at the B3LYP/6-31G* level are described later in this paper. The potential-energy surface demonstrates the nonsynchronous and nonconcerted reaction pathway. The synchronous pathway (diagonal in Figure 3) is strongly disfavored.

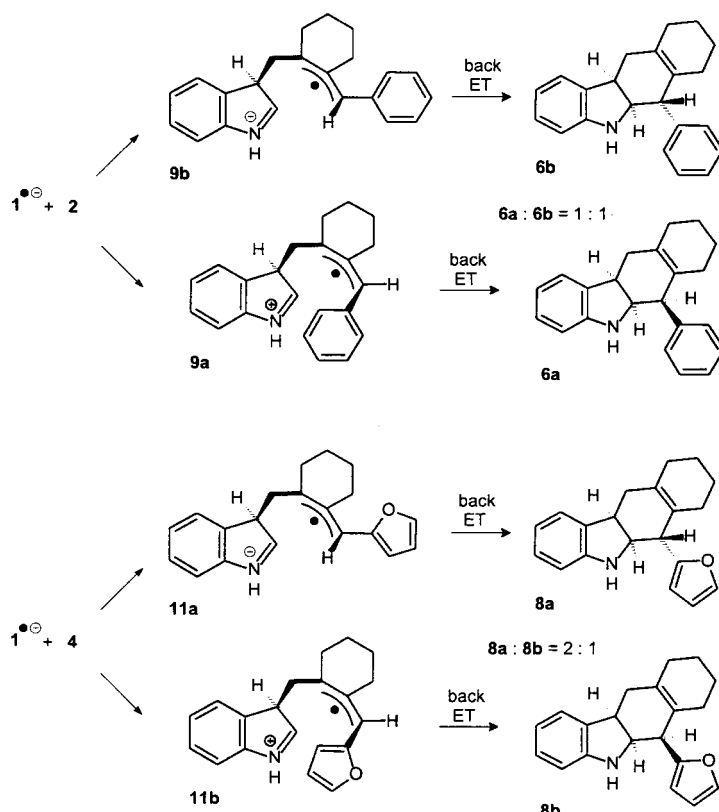
In earlier investigations, we demonstrated that indole is oxidized to its radical cation under the reaction conditions described here. *Ab initio* calculations showed that the indole radical cation is planar with a high positive charge in the 2-position, whereas the radical character is mainly localized in the 3-position.^[8] The minimum-energy reaction pathway on the potential-energy surface demonstrates that the first formed bond is the y bond in Scheme 2. This is equivalent to an attack of the diene to the reactive 3-position of the indole radical cation. That the attack proceeds in this position can be rationalized by the more favourable delocalization in **9**, leading to a distonic immonium ion/allyl radical intermediate. The calculated highest spin densities are located at the allylic system conjugated with the phenyl ring as indicated in Figure 4. These results are also confirmed by the *ab initio* and B3LYP calculations given below. These intermediates are sometimes called “long-bond” intermediates with regard to the developing x bond indicated in Scheme 2.^[9b] However, as Figure 3 demonstrates, the valley for the long-bond intermediates at the potential-energy surface is very much elongated.

Ab initio and DFT calculations of the intermediates: To verify the reliability of the potential-energy hypersurface obtained

Figure 4. Spin densities in the distonic radical-cation intermediate **9a**. The isosurface plot represents the highest spin density.

by semiempirical calculations, the energies of all long-bond intermediates, have been recalculated by molecular orbital and density functional (DFT) methods. First, we examined the regioselectivity of the reaction. For all possible regioisomers, we calculated the energies of the distonic radical-cation

intermediates. The potential-energy surfaces show that a reaction path leading to an intermediate with a lower energy proceeds with a low activation-energy barrier, whereas pathways to intermediates with relatively high energy afford higher activation energies. Although the absolute energies and barrier heights calculated by the semiempirical methods may not be accurate, comparison of the relative energies of the regioisomeric intermediates allows the prediction of the preferred regioisomer. Our B3LYP/6-31G*//UHF/6-31G* calculations of the different possible intermediates demonstrate that only the attack of the unsubstituted exocyclic methylene group of the diene to the 3-position of the indole radical cation leads to intermediates with lower energies (e.g., **9a**, **9b**, **11a**, **11b**; Scheme 3), whereas an attack of the substituted position of the exocyclic diene is highly disfavored and leads to intermediates that are more than 10 kcal mol⁻¹ higher in energy. This regioselectivity can also be explained by the fact that only the isomeric intermediates **9a**, **9b**, **11a**, and **11b** have a conjugation of the allylic radical with the phenyl system; this lowers the energy of the intermediates and the

Scheme 3. Stereochemistry of the reactions between **1•+** and **2** and between **1•+** and **4**.

transition states significantly. An example of one of these intermediates and a plot of the spin density of this radical cation is shown in Figure 4. This demonstrates the character of the intermediate as an allyl/benzyl radical. The structures **9a**, **9b**, **11a**, and **11b** in Scheme 3 represent the energetically preferred *exo* attack of the exocyclic dienes to the indole radical cation. Corresponding calculations for the opposite *endo* approach leads to intermediates which are higher in energy by 4 kcal mol⁻¹ relative to the *exo* attack shown in Figures 3 and 4.

The energy difference between the stereoisomers **9a** and **9b** (Scheme 3) is less than 1 kcal mol⁻¹; this explains why the ratio of the products **6a** and **6b** was found to be 1:1. Applying this reaction model to the furyl-substituted system, we could predict the preference for diastereomer **8a**. The energies of the long-bond intermediates **11a** and **11b** leading to the diastereoisomers **8a** and **8b** were calculated at the UHF/AM1, UHF/3-21G, UHF/6-31G*, and B3LYP/6-31G* levels of theory. The UHF/6-31G* optimized structures of **11a** and **11b** are shown in Figure 5. In all calculations, **11a** is the

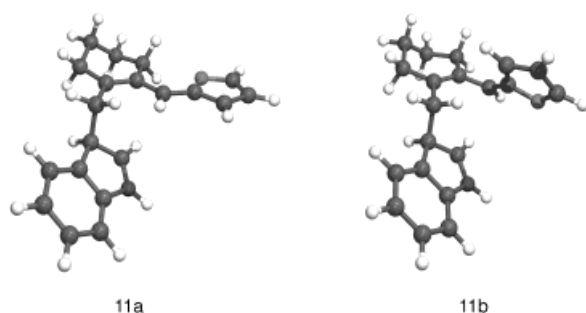


Figure 5. The optimized structures of the distonic radical-cation intermediates **11a** and **11b**.

preferred intermediate leading to **8a**. This is in excellent agreement with the results of the subsequently performed reaction between indole and **4** leading to **8a** as the preferred diastereomer (**8a**:**8b** = 2:1). The energies of the two possible intermediates, calculated with various quantum-chemical methods, are shown in Table 1.

Table 1. Energy differences between the intermediates **11a** and **11b**, calculated with different quantum-chemical methods in kcal mol⁻¹. In every case, **11a** is lower in energy.

	$E(\mathbf{11b}) - E(\mathbf{11a})$ [kcal mol ⁻¹]
UHF/AM1//UHF/AM1	2.5
UHF/3-21G//UHF/AM1	4.7
UHF/3-21G//UHF/3-21G	7.4
UHF/6-31G*//UHF/6-31G*	4.5
Becke3LYP/6-31G*//UHF/6-31G*	5.0

Conclusions

Electron-transfer-induced Diels–Alder reactions of indole with aromatic- or heteroaromatic-substituted exocyclic dienes proceed with complete regioselectivity to form [*b*]-annelated tetrahydrocarbazoles. For this reaction, the results of the

calculations of the potential-energy surface and the distonic radical-cation intermediates are in very good agreement with the experimental results and the proposed mechanism. Though the approximation of free, unsolvated radical cations is made, the regio- and diastereoselectivities can be rationalized and predicted properly. Quantum-chemical calculations lead to a reaction model that is consistent with the observed products. The good agreement of the results from the computationally efficient B3LYP method with the experimental results also encourages the investigation and prediction of other electron-transfer-induced cycloadditions. These studies are currently in process and will be reported in due course.

Computational Methodology

In the last years, hybrid density functional methods such as the B3LYP functional gave results in excellent agreement with the available experimental data and highly correlated MO-based methods.^[14, 15] In an earlier publication, we could show that this method is a very promising tool for the study of radical-ion and other open-shell reactions.^[16] In a recent study of the radical-cation Diels–Alder reaction between 1,3-butadiene and ethylene at high levels of theory, we could demonstrate that there is a good agreement of Becke3LYP results with QCISD(T) calculations.^[17] This indicates that these computationally efficient methods can also be used in investigations of larger model systems of radical-cationic reaction mechanisms. We therefore adopted a computational strategy in which the structures were, except where noted, fully optimized and characterized at the B3LYP/6-31G*//UHF/6-31G* level of theory.^[18, 19]

The complete potential-energy surfaces were calculated with the semiempirical UHF/AM1 method, which was preferred to PM3 since the latter predicts unrealistic partial charges on nitrogen atoms, whereas AM1 provides reliable results for aromatic compounds and radical cations. The calculations of the energy surfaces were carried out with complete geometry optimization on every point. All semiempirical calculations were performed by the Hyperchem 5 program.^[20]

The ab initio and DFT calculations were performed using the GAUSSIAN 94 series of programs^[21] running on IBM SP1/SP2 and SGI Origin parallel computers at the High Performance Computing Cluster at the University of Notre Dame.

Experimental Section

General: Solvents were purified and dried by literature procedures. Reagents were employed as purchased. Thin-layer chromatography (TLC) was carried out on aluminium sheets, precoated with silica gel 60 F₂₅₄ (Merck). For liquid chromatography, flash silica gel 30–60 μm (Baker) was used. Melting points were recorded on a Reichert (Wien) melting point apparatus and are uncorrected. Mass spectra and high-resolution MS were taken with an AEI (Manchester) MS 50 instrument and a Finnigan MAT 312 spectrometer by EI (70 eV). ¹H NMR and ¹³C NMR spectra were recorded on Bruker AC200 and AM400 instruments. Chemical shifts (δ) are reported relative to tetramethylsilane (TMS) or CDCl₃ as references. Irradiation was performed using a 450 W xenon arc lamp (Osram XBO-450 OFR) incorporated into a lamp-housing LAX 1450 (Müller Elektronik, Moosinning) equipped with a long-pass filter 5146 (λ > 345 nm, Oriel, Stanford).

Materials: 2,4,6-trianisylpyrylium tetrafluoroborate (**5**) was prepared according to the literature.^[22] The exocyclic dienes **2**, **3**, and **4** were synthesized by Wittig reactions between the corresponding ketones and methyl triphenylphosphonium bromide according to equivalent preparations in the literature.^[23] The corresponding ketones were synthesized from cyclohexanone by aldol reactions with the corresponding aromatic aldehydes or furfural according to literature procedures.^[24]

General procedure for the photoinduced electron-transfer-initiated Diels–Alder reactions: The exocyclic diene **2**, **3**, or **4**, the equivalent amount of indole (**1**), and the pyrylium salt **5** (2 mol %) as a sensitizer were placed in a Schlenk tube and dry dichloromethane (70 mL) was added. The solution was freed from oxygen under an argon stream by ultrasonic treatment for 10 min. The mixture was then irradiated for the indicated times with water cooling (10–15 °C) at a wavelength of $\lambda > 345$ nm. After the irradiation, the pyrylium salt was separated from the products on a short silica filtration column with dichloromethane as the eluent. Separation and isolation was carried out as indicated for the different products.

6-Phenyl-5a,6,7,8,9,10,11,11a-octahydrobenzo[*b*]carbazole (6a and 6b): As described in the general procedure, irradiation of indole (**1**, 234 mg, 2 mmol) and benzylidene-2-methylenecyclohexane (**2**, 369 mg, 2 mmol) was performed for 24 h. Work-up and separation of the reaction mixture by flash chromatography on silica (cyclohexane/diethyl ether 25:1 as the eluent) gave 84.1 mg of **6a** and 84.4 mg of **6b** with a total yield of 28%.

Compound 6a: White solid; m.p. 93 °C; ¹H NMR (400 MHz, CDCl₃, 25 °C): $\delta = 7.29$ (m, 5H; CH), 7.11 (d, ³J(H,H) = 7.5 Hz, 1H; CH), 7.05 (ddd, ³J(H,H) = 7.7, 7.4 Hz, ⁵J(H,H) = 1.1 Hz, 1H; CH), 6.77 (ddd, ³J(H,H) = 7.5, 7.4 Hz, ⁵J(H,H) = 1.1 Hz, 1H; CH), 6.65 (d, ³J(H,H) = 7.7 Hz, 1H; CH), 3.94 (dd, ³J(H,H) = 8.1, 5.6 Hz, 1H; CH), 3.45 (td, ³J(H,H) = 8.5, 8.1 Hz, 1H; CH), 3.25 (d, ³J(H,H) = 5.6 Hz, 1H; CH), 2.52 (dd, ²J(H,H) = 17.1 Hz, ³J(H,H) = 8.5 Hz, 1H; CH₂), 2.26 (d, ²J(H,H) = 17.1 Hz, 1H; CH₂), 2.06 (br, 2H; CH₂), 1.60 (m, 6H; CH₂); ¹³C NMR (50.3 MHz, CDCl₃, 25 °C): $\delta = 149.9$ (C), 142.9 (C), 134.6 (C), 130.0 (C), 128.9 (CH), 128.5 (CH), 128.0 (C), 127.3 (CH), 126.5 (CH), 123.4 (CH), 119.0 (CH), 110.0 (CH), 65.9 (CH), 50.2 (CH), 37.8 (CH), 33.0 (CH₂), 30.8 (CH₂), 29.0 (CH₂), 23.3 (CH₂), 23.0 (CH₂); MS (70 eV, EI): *m/z* (%): 301 (15) [*M*⁺], 184 (55) [retro-DA], 141 (47), 117 (100) [retro-DA], 91 (11) [C₇H₇⁺], 77 (8) [C₆H₅⁺]; HR-MS calcd for C₂₂H₂₃N 301.1831, found 301.1836.

Compound 6b: White solid; m.p. 94 °C; ¹H NMR (400 MHz, CDCl₃, 25 °C): $\delta = 7.30$ (m, 5H; CH), 7.13 (dd, ³J(H,H) = 7.2 Hz, ⁵J(H,H) = 1.2 Hz, 1H; CH), 6.95 (ddd, ³J(H,H) = 7.7, 7.6 Hz, ⁵J(H,H) = 1.2 Hz, 1H; CH), 6.70 (ddd, ³J(H,H) = 7.6, 7.2 Hz, ⁵J(H,H) = 1.0 Hz, 1H; CH), 6.45 (dd, ³J(H,H) = 7.7 Hz, ⁵J(H,H) = 1.0 Hz, 1H; CH), 4.08 (dd, ³J(H,H) = 6.45 Hz, 1H; CH), 3.63 (d, ³J(H,H) = 6.45 Hz, 1H; CH), 3.19 (dt, ³J(H,H) = 7.8, 6.45 Hz, 1H; CH), 3.00 (br, 1H; CH), 2.09 (d, ³J(H,H) = 7.8 Hz, 2H; CH₂), 2.04 (br, 2H; CH₂), 1.68 (m, 6H; CH₂); ¹³C NMR (50.3 MHz, CDCl₃, 25 °C): $\delta = 149.5$ (C), 141.4 (C), 136.0 (C), 130.7 (C), 129.8 (CH), 128.1 (CH), 127.2 (C), 127.1 (CH), 126.4 (CH), 123.0 (CH), 118.7 (CH), 109.8 (CH), 63.5 (CH), 49.1 (CH), 39.1 (CH), 33.2 (CH₂), 31.0 (CH₂), 28.8 (CH₂), 23.5 (CH₂), 23.2 (CH₂); MS (70 eV, EI): *m/z* (%): 301 (18) [*M*⁺], 256 (6), 184 (57) [retro-DA], 141 (52), 117 (100) [retro-DA], 91 (12) [C₇H₇⁺], 77 (8) [C₆H₅⁺]; HR-MS calcd for C₂₂H₂₃N 301.1831, found 301.1836.

6-Anisyl-5a,6,7,8,9,10,11,11a-octahydrobenzo[*b*]carbazole (7a and 7b): As described in the general procedure, irradiation of indole (**1**, 117 mg, 1 mmol) and (4'-methoxybenzylidene)-2-methylenecyclohexane (**3**, 214 mg, 1 mmol) was performed for 8 h. Work-up and separation of the reaction mixture by flash chromatography on silica (cyclohexane/diethyl ether 7:1 as the eluent) gave 55.5 mg of **7a** and 63.8 mg of **7b** with a total yield of 36%.

Compound 7a: White solid; m.p. 117 °C; ¹H NMR (400 MHz, CDCl₃, 25 °C): $\delta = 7.18$ (d, ³J(H,H) = 8.6 Hz, 2H; CH), 7.10 (d, ³J(H,H) = 7.3 Hz, 1H; CH), 6.99 (dd, ³J(H,H) = 7.8, 7.6 Hz, 1H; CH), 6.88 (d, ³J(H,H) = 8.6 Hz, 2H; CH), 6.78 (dd, ³J(H,H) = 7.6, 7.3 Hz, 1H; CH), 6.68 (d, ³J(H,H) = 7.8 Hz, 1H; CH), 3.93 (dd, ³J(H,H) = 8.0, 6.2 Hz, 1H; CH), 3.46 (dt, ³J(H,H) = 8.0, 7.4 Hz, 1H; CH), 2.86 (d, ³J(H,H) = 6.2 Hz, 1H; CH), 2.40 (br, 2H; CH₂), 2.05 (m, 2H; CH₂), 1.66 (m, 6H; CH₂); ¹³C NMR (100.6 MHz, CDCl₃, 25 °C): $\delta = 158.3$ (C), 149.8 (C), 137.8 (C), 134.7 (C), 130.8 (CH), 130.5 (C), 128.3 (C), 127.2 (CH), 123.5 (CH), 119.0 (CH), 113.7 (CH), 110.0 (CH), 65.9 (CH), 55.3 (CH₃), 49.3 (CH), 37.7 (CH), 33.0 (CH₂), 29.1 (CH₂), 28.6 (CH₂), 23.3 (CH₂), 23.1 (CH₂); MS (70 eV, EI): *m/z* (%): 331 (15) [*M*⁺], 214 (100) [retro-DA], 183 (31), 171 (63), 141 (15), 117 (17) [retro-DA], 91 (4) [C₇H₇⁺]; HR-MS calcd for C₂₃H₂₅NO 331.1936, found 331.1938.

Compound 7b: White solid; m.p. 119 °C; ¹H NMR (400 MHz, CDCl₃, 25 °C): $\delta = 7.17$ (d, ³J(H,H) = 8.6 Hz, 2H; CH), 7.12 (d, ³J(H,H) = 7.3 Hz, 1H; CH), 6.96 (dd, ³J(H,H) = 7.7, 7.5 Hz, 1H; CH), 6.88 (d, ³J(H,H) = 8.6 Hz, 2H; CH), 6.71 (dd, ³J(H,H) = 7.5, 7.3 Hz, 1H; CH), 6.49 (d,

³J(H,H) = 7.7 Hz, 1H; CH), 4.07 (dd, ³J(H,H) = 6.2 Hz, 1H; CH), 3.60 (d, ³J(H,H) = 6.2 Hz, 1H; CH), 3.20 (td, ³J(H,H) = 7.4, 6.2 Hz, 1H; CH), 2.10 (br, 2H; CH₂), 2.03 (m, 2H; CH₂), 1.65 (m, 6H; CH₂); ¹³C NMR (100.6 MHz, CDCl₃, 25 °C): $\delta = 158.2$ (C), 149.5 (C), 136.1 (C), 133.4 (C), 130.6 (CH), 130.5 (C), 127.5 (C), 127.1 (CH), 123.1 (CH), 118.7 (CH), 113.5 (CH), 109.8 (CH), 63.7 (CH), 55.3 (CH₃), 48.2 (CH), 39.0 (CH), 33.2 (CH₂), 31.1 (CH₂), 28.8 (CH₂), 23.5 (CH₂), 23.2 (CH₂); MS (70 eV, EI): *m/z* (%): 331 (13) [*M*⁺], 286 (7), 214 (100) [retro-DA], 183 (32), 171 (57), 141 (18), 117 (28) [retro-DA], 77 (8) [C₆H₅⁺]; HR-MS calcd for C₂₃H₂₅NO 331.1936, found 331.1940.

6-(Furan-2-yl)-5a,6,7,8,9,10,11,11a-octahydrobenzo[*b*]carbazole (8a and 8b): As described in the general procedure, irradiation of indole (**1**, 117 mg, 1 mmol) and (furan-2-yl-methylene)-2-methylenecyclohexane (**4**, 174 mg, 1 mmol) was performed for 7 h. Work-up and separation of the reaction mixture by flash chromatography on silica (cyclohexane/diethyl ether 7:1 as the eluent) gave 89.1 mg of **8a** and 45.2 mg of **8b** with a total yield of 46%.

Compound 8a: White solid; m.p. 90 °C; ¹H NMR (500 MHz, CDCl₃, 25 °C): $\delta = 7.36$ (dd, *J* = 1.9, 0.9 Hz, 1H; CH), 7.04 (d, ³J(H,H) = 7.5 Hz, 1H; CH), 6.96 (dd, ³J(H,H) = 7.6, 7.5 Hz, 1H; CH), 6.68 (ddd, ³J(H,H) = 7.5, 7.5 Hz, ⁵J(H,H) = 1.0 Hz, 1H; CH), 6.54 (d, ³J(H,H) = 7.6 Hz, 1H; CH), 6.27 (dd, *J* = 3.2, 1.9 Hz, 1H; CH), 6.03 (d, *J* = 3.2 Hz, 1H; CH); 4.25 (dd, ³J(H,H) = 8.3, 5.5 Hz, 1H; CH), 3.64 (d, ³J(H,H) = 5.5 Hz, 1H; CH), 3.52 (dt, ³J(H,H) = 8.3, 8.0 Hz, 1H; CH), 2.37 (d, ³J(H,H) = 8.0 Hz, 2H; CH₂), 2.00 (m, 2H; CH₂), 1.70 (m, 6H; CH₂); ¹³C NMR (100.6 MHz, CDCl₃, 25 °C): $\delta = 155.1$ (C), 150.4 (C), 141.5 (CH), 134.4 (C), 131.1 (C), 127.4 (CH), 127.1 (C), 122.8 (CH), 118.4 (CH), 110.0 (CH), 109.0 (CH), 107.6 (CH), 62.4 (CH), 43.0 (CH), 39.7 (CH), 33.4 (CH₂), 31.0 (CH₂), 28.6 (CH₂), 23.3 (CH₂), 23.0 (CH₂); MS (70 eV, EI): *m/z* (%): 291 (11) [*M*⁺], 174 (100) [retro-DA], 145 (32), 132 (29), 117 (50) [retro-DA], 91 (16) [C₇H₇⁺], 77 (13) [C₆H₅⁺]; HR-MS calcd for C₂₂H₂₃N 291.1623, found 291.1625.

Compound 8b: White solid; m.p. 92 °C; ¹H NMR (400 MHz, CDCl₃, 25 °C): $\delta = 7.43$ (dd, *J* = 1.8, 0.8 Hz, 1H; CH), 7.12 (d, ³J(H,H) = 7.4 Hz, 1H; CH), 7.07 (d, ³J(H,H) = 7.5 Hz, 1H; CH), 6.64 (d, ³J(H,H) = 7.5 Hz, 1H; CH), 6.69 (ddd, ³J(H,H) = 7.5, 7.4 Hz, ⁵J(H,H) = 1.0 Hz, 1H; CH), 6.37 (dd, *J* = 3.2, 1.8 Hz, 1H; CH), 6.15 (d, *J* = 3.2 Hz, 1H; CH), 4.16 (dd, ³J(H,H) = 8.8, 6.6 Hz, 1H; CH), 3.59 (dt, ³J(H,H) = 8.8, 7.9 Hz, 1H; CH), 3.36 (d, ³J(H,H) = 6.6 Hz, 1H; CH), 2.56 (d, ³J(H,H) = 7.9 Hz, 2H; CH₂), 1.95 (m, 2H; CH₂), 1.65 (m, 6H; CH₂); ¹³C NMR (100.6 MHz, CDCl₃, 25 °C): $\delta = 155.6$ (C), 150.2 (C), 141.9 (CH), 1333.6 (C), 130.4 (C), 127.6 (CH), 127.0 (C), 123.6 (CH), 118.9 (CH), 109.7 (CH), 109.0 (CH), 107.4 (CH), 62.1 (CH), 44.3 (CH), 38.9 (CH), 32.7 (CH₂), 30.7 (CH₂), 27.9 (CH₂), 23.2 (CH₂), 22.9 (CH₂); MS (70 eV, EI): *m/z* (%): 291 (18) [*M*⁺], 174 (100) [retro-DA], 145 (24), 132 (21), 117 (32) [retro-DA], 91 (11) [C₇H₇⁺], 77 (8) [C₆H₅⁺]; HR-MS calcd for C₂₂H₂₃N 291.1623, found 291.1626.

Acknowledgment

Financial support provided by the Volkswagen Stiftung (Grants I/71 748 to E.S. and I/72 647 to O.W.), the Fonds der Chemischen Industrie, and the BASF Aktiengesellschaft is gratefully acknowledged. We are grateful to the Office of Information Technologies at the University of Notre Dame for generous allocation of computing resources.

- [1] a) F. Müller, J. Mattay, *Chem. Rev.* **1993**, 93, 99; b) N. L. Bauld, *Tetrahedron* **1989**, 45, 5307; c) H. Chanon, L. Ebersson, in *Photoinduced Electron Transfer Reactions* (Eds.: M. A. Fox, M. Chanon), Elsevier, Amsterdam **1988**, p. 409; d) J. Mattay, G. Trampe, J. Runsink, *Chem. Ber.* **1988**, 121, 1991; e) N. L. Bauld, D. J. Bellville, B. Harirchian, K. T. Lorenz, R. A. Pabon, D. W. Reynolds, D. D. Wirth, H. S. Chiou, B. K. Marsh, *J. Am. Chem. Soc.* **1987**, 109, 371; f) M. Schmittl, A. Burghart, *Angew. Chem.* **1997**, 109, 2659; *Angew. Chem. Int. Ed. Engl.* **1997**, 36, 2550.
- [2] a) J. Botzem, U. Haberl, E. Steckhan, S. Blechert, *Acta Chem. Scand.* **1998**, 52, 175; b) T. Peglow, S. Blechert, E. Steckhan, *Chem. Eur. J.* **1998**, 4, 107; c) C. F. Gürtler, E. Steckhan, S. Blechert, *J. Org. Chem.* **1996**, 61, 4136; d) C. F. Gürtler, E. Steckhan, S. Blechert, *Synlett* **1994**,

- 141; e) C. F. Gürtler, E. Steckhan, S. Blechert, *Angew. Chem.* **1995**, *107*, 2025; *Angew. Chem. Int. Ed. Engl.* **1995**, *34*, 1900.
- [3] B. Harirchian, N. L. Bauld, *J. Am. Chem. Soc.* **1989**, *111*, 1826.
- [4] a) F. Wenkert, P. D. R. Moeller, S. R. Piettre, *J. Am. Chem. Soc.* **1988**, *110*, 7188; b) G. A. Kraus, D. Bougie, *J. Org. Chem.* **1989**, *54*, 2425.
- [5] a) O. Wiest, E. Steckhan, *Angew. Chem.* **1993**, *105*, 932; *Angew. Chem. Int. Ed. Engl.* **1993**, *32*, 901; b) O. Wiest, E. Steckhan, *Tetrahedron Lett.* **1993**, *34*, 6391; c) A. Gieseler, E. Steckhan, O. Wiest, F. Knoch, *J. Org. Chem.* **1991**, *56*, 105; d) A. Gieseler, E. Steckhan, O. Wiest, *Synlett* **1990**, 275.
- [6] a) U. Pindur, M. Haber, H. Erfanian-Abdoust, *Heterocycles* **1992**, *34*, 781; b) U. Pindur, M. Haber, K. Sattler, *J. Chem. Educ.* **1993**, *70*, 263.
- [7] a) K. T. Lorenz, N. L. Bauld, *J. Am. Chem. Soc.* **1987**, *109*, 1157; b) D. W. Reynolds, K. T. Lorenz, H. S. Chiou, D. J. Bellville, R. A. Pabon, N. L. Bauld, *J. Am. Chem. Soc.* **1987**, *109*, 4960; c) P. G. Gassmann, D. A. Singleton, *J. Am. Chem. Soc.* **1984**, *106*, 7993.
- [8] O. Wiest, E. Steckhan, F. Grein, *J. Org. Chem.* **1992**, *57*, 4034.
- [9] a) N. L. Bauld, D. J. Bellville, R. A. Pabon, R. Chelsky, G. J. Green, *J. Am. Chem. Soc.* **1983**, *105*, 2378; b) D. J. Bellville, N. L. Bauld, R. A. Pabon, S. A. Gardner, *J. Am. Chem. Soc.* **1983**, *105*, 3584.
- [10] N. L. Bauld, *J. Am. Chem. Soc.* **1992**, *114*, 5800.
- [11] a) D. J. Bellville, N. L. Bauld, *J. Am. Chem. Soc.* **1982**, *104*, 2665; b) D. J. Bellville, N. L. Bauld, *Tetrahedron* **1986**, *42*, 6167.
- [12] J. Ilcoch, E. Steckhan, *Tetrahedron Lett.* **1987**, *27*, 1081.
- [13] a) M. Schmittel, C. Wöhrle, I. Bohn, *Chem. Eur. J.* **1996**, *2*, 1031; b) M. Schmittel, C. Wöhrle, I. Bohn, *Acta Chem. Scand.* **1997**, *51*, 151.
- [14] a) J. Wang, A. D. Becke, V. H. Smith, Jr., *J. Chem. Phys.* **1995**, *102*, 3477; b) G. J. Laming, N. Handy, R. D. Amos, *Mol. Phys.* **1993**, *80*, 1121.
- [15] a) T. Clark, *Top. Curr. Chem.* **1996**, *177*, 1; b) C. W. Murray, N. Handy, *J. Chem. Phys.* **1992**, *97*, 6509; c) N. C. Handy, N. L. Ma, B. J. Smith, J. A. Pople, L. Radom, *J. Am. Chem. Soc.* **1991**, *113*, 7903.
- [16] O. Wiest, *J. Am. Chem. Soc.* **1997**, *119*, 5713.
- [17] U. Haberl, O. Wiest, E. Steckhan, *J. Am. Chem. Soc.* **1999**, *121*, 6730.
- [18] A. D. Becke, *J. Chem. Phys.* **1993**, *98*, 5648.
- [19] C. Lee, W. Yang, R. G. Parr, *Phys. Rev. B.* **1988**, *37*, 786.
- [20] *Hyperchem 5.0*, Hypercube, Ontario, **1996**.
- [21] M. J. Frisch, G. W. Trucks, H. B. Schlegel, P. M. W. Gill, B. G. Johnson, M. A. Robb, J. R. Cheeseman, T. Keith, G. A. Petersson, J. A. Montgomery, K. Raghavachari, M. A. I-Laham, V. G. Zakrzewski, J. V. Ortiz, J. B. Foresman, C. Y. Peng, P. Y. Ayala, W. Chen, M. W. Wong, J. L. Andres, E. S. Replogle, R. Gomperts, R. L. Martin, D. J. Fox, J. S. Binkley, D. J. Defrees, J. Baker, J. P. Stewart, M. Head-Gordon, C. Gonzalez, J. A. Pople, *Gaussian 94*, Gaussian, Pittsburgh, PA, **1995**.
- [22] M. Martiny, E. Steckhan, T. Esch, *Chem. Ber.* **1993**, *126*, 1671.
- [23] R. J. Olsen, J. C. Minniear, W. M. Overton, J. M. Sherrick, *J. Org. Chem.* **1991**, *56*, 989.
- [24] a) H. M. Walton, *J. Org. Chem.* **1957**, *22*, 1161; b) H. O. House, R. L. Wasson, *J. Am. Chem. Soc.* **1956**, *78*, 4394.

Received: February 15, 1999 [F1616]